AMERICAN SOCIETY FOR MICROBIOLOGY | Journal of Bacteriology®

RESEARCH ARTICLE

Regulation of the CRISPR-Associated Genes by Rv2837c (CnpB) via an Orn-Like Activity in Tuberculosis Complex Mycobacteria

Yang Zhang,[a]* Jun Yang,[a] Guangchun Bai[a]

[a]Department of Immunology and Microbial Disease, Albany Medical College, Albany, New York, USA

ABSTRACT Clustered regularly interspaced short palindromic repeats (CRISPR) and the CRISPR-associated proteins (Cas) provide bacteria and archaea with adaptive immunity to specific DNA invaders. *Mycobacterium tuberculosis* encodes a type III CRISPR-Cas system that has not been experimentally explored. In this study, we found that the CRISPR-Cas systems of both *M. tuberculosis* and *Mycobacterium bovis* BCG were highly upregulated by deletion of Rv2837c (*cnpB*), which encodes a multifunctional protein that hydrolyzes cyclic di-AMP (c-di-AMP), cyclic di-GMP (c-di-GMP), and nanoRNAs (short oligonucleotides of 5 or fewer residues). By using genetic and biochemical approaches, we demonstrated that the CnpB-controlled transcriptional regulation of the CRISPR-Cas system is mediated by an Orn-like activity rather than by hydrolyzing the cyclic dinucleotides. Additionally, our results revealed that tuberculosis (TB) complex mycobacteria are functional in processing CRISPR RNAs (crRNAs), which are also more abundant in the Δ*cnpB* strain than in the parent strain. The elevated crRNA levels in the Δ*cnpB* strain could be partially reduced by expressing *Escherichia coli orn*. Our findings provide new insight into transcriptional regulation of bacterial CRISPR-Cas systems.

IMPORTANCE Clustered regularly interspaced short palindromic repeats (CRISPR) and the CRISPR-associated proteins (Cas) provide adaptive immunity to specific DNA invaders. *M. tuberculosis* encodes a type III CRISPR-Cas system that has not been experimentally explored. In this study, we first demonstrated that the CRISPR-Cas systems in tuberculosis (TB) complex mycobacteria are functional in processing CRISPR RNAs (crRNAs). We also showed that Rv2837c (CnpB) controls the expression of the CRISPR-Cas systems in TB complex mycobacteria through an oligoribonuclease (Orn)-like activity, which is very likely mediated by nanoRNA. Since little is known about regulation of CRISPR-Cas systems, our findings provide new insight into transcriptional regulation of bacterial CRISPR-Cas systems.

KEYWORDS *Mycobacterium tuberculosis*, Rv2837c, Orn, CRISPR, nanoRNA, c-di-AMP

Clustered regularly interspaced short palindromic repeats (CRISPR) and the CRISPR-associated (*cas*) genes have been discovered in approximately one-half of bacteria and most archaea that have been sequenced (1–3). The CRISPR-Cas systems provide these cells with prokaryotic adaptive immunity to invasion of mobile genetic elements, including plasmids and viruses (1–3). CRISPRs harbor arrays of conserved short repetitive DNA sequences (repeats), which are interspaced by unique DNA fragments (spacers) adapted from foreign invaders. The *cas* genes are typically clustered in an operon adjacent to the CRISPR arrays. The proteins encoded by these genes include nucleases, helicases, DNA- and RNA-binding proteins, and polymerases (4). Traditionally, CRISPR-Cas systems have been classified into three major types (5, 6). A new classification was expanded to encompass six types, among which types I, II, and III have been extensively studied (6–8).

The CRISPR-Cas system-mediated defense process can be divided into three phases:

Received 8 December 2017 **Accepted** 25 January 2018

Accepted manuscript posted online 29 January 2018

Citation Zhang Y, Yang J, Bai G. 2018. Regulation of the CRISPR-associated genes by Rv2837c (CnpB) via an Orn-like activity in tuberculosis complex mycobacteria. J Bacteriol 200:e00743-17. https://doi.org/10.1128/JB.00743-17.

Editor George O'Toole, Geisel School of Medicine at Dartmouth

Address correspondence to Guangchun Bai, baig@mail.amc.edu.

* Present address: Yang Zhang, Shanghai Institute for Advanced Immunochemical Studies, Shanghai, China.

(i) spacer acquisition, (ii) CRISPR expression, and (iii) CRISPR interference (1–3). The components of bacterial CRISPR-Cas systems and their roles in gene editing have been extensively characterized in recent years. In contrast, transcriptional regulation of CRISPR-Cas systems is overall poorly understood. In several bacterial species, CRISPR-Cas systems are regulated by transcription factors, such as cyclic AMP (cAMP) receptor protein (CRP), histone-like nucleoid-structuring (H-NS) protein, leucine-responsive regulatory protein (LRP), and regulator of leucine biosynthesis operon (LeuO) (9–15).

Mycobacterium tuberculosis is the etiologic agent of tuberculosis (TB), which causes approximately 8 to 9 million new cases and around 1.5 million deaths annually according to the recent annual TB reports of the World Health Organization (WHO). Although *M. tuberculosis* has been recognized for over a century, the biology of the pathogen remains largely unknown. The CRISPR-Cas systems in mycobacteria have been bioinformatically analyzed (16, 17), whereas the biology of these systems has not been experimentally explored in TB complex mycobacteria. *M. tuberculosis* encodes a type III CRISPR-Cas system, which is composed of two CRISPR arrays that harbor 24 and 18 repeats, respectively. The 36-bp repeat sequences in both CRISPR arrays are highly conserved among TB complex mycobacteria. The arrangement of the CRISPR arrays of *Mycobacterium bovis* is similar to that of *M. tuberculosis* except that *M. bovis* consists of 25 and 17 repeats, respectively, within the two CRISPR arrays. *Mycobacterium bovis* BCG (BCG) was originally derived from *M. bovis* and is the currently available attenuated vaccine strain against *M. tuberculosis*. BCG harbors 30 and 19 repeats, respectively, within the two CRISPR arrays (16). Therefore, BCG possesses several distinct spacers compared to both *M. tuberculosis* and *M. bovis*.

We have previously reported that *M. tuberculosis* Rv3586 (*disA*) encodes a diadenylate cyclase that converts ATP into cyclic di-AMP (c-di-AMP) (18). *M. tuberculosis* Rv2837c (*cnpB*) encodes a phosphodiesterase that specifically cleaves c-di-AMP into AMP (19). We also demonstrated that DisA is the sole diadenylate cyclase in *M. tuberculosis*, as a Δ*disA* Δ*cnpB* strain does not process detectable c-di-AMP (20). Deletion of *cnpB* resulted in significant virulence attenuation in a mouse pulmonary infection model (19, 21), which was very likely due to significantly elevated c-di-AMP levels, as overexpression of *M. tuberculosis disA* also led to a similar outcome (22). An earlier study demonstrated that CnpB functions similarly to an *Escherichia coli* oligoribonuclease (Orn) that hydrolyzes 2-mer to 5-mer nanoRNAs (short oligonucleotides of 5 or fewer residues), except that CnpB prefers 2-mer nanoRNA as a substrate (23). Additionally, a recent report showed that CnpB also degrades cyclic di-GMP (c-di-GMP) (24), although we showed that CnpB prefers c-di-AMP to c-di-GMP, according to an *in vitro* enzymatic kinetics analysis (19). In this study, we performed a transcriptome-sequencing (RNA-Seq) analysis using *M. tuberculosis* wild type (WT) and Δ*cnpB* to determine genes that were differentially expressed between the two strains. Surprisingly, we found that the RNA reads of the CRISPR-Cas system in the Δ*cnpB* strain were much higher than those in the WT. We further determined the molecular basis of the CnpB-mediated control of the CRISPR-Cas systems in TB complex mycobacteria. Our findings reveal that CnpB controls the CRISPR-Cas systems through an Orn-like activity, which is very likely mediated by nanoRNA rather than by hydrolyzing c-di-AMP or c-di-GMP.

RESULTS

RNA-Seq analysis revealed that CnpB controls expression of the CRISPR-Cas systems in *M. tuberculosis* and BCG in a c-di-AMP-independent manner. We have previously shown that *M. tuberculosis* CnpB is functional as a c-di-AMP phosphodiesterase and that deletion of *cnpB* significantly elevates c-di-AMP levels within *M. tuberculosis* (19). In this study, we initially attempted to determine c-di-AMP-mediated gene regulation in *M. tuberculosis* by comparing the expression profiles of the WT and Δ*cnpB* strains using RNA-Seq. Overall, 26 genes were upregulated and 35 genes were downregulated significantly in the mutant compared to the WT, using ≥2 -fold change as a cutoff (Table 1). Interestingly, all the *cas* genes were highly upregulated in the Δ*cnpB* strain compared to the WT (Fig. 1A and B). It has been reported that the *M.*

TABLE 1 Gene regulation by deletion of *cnpB* in *M. tuberculosis*[a]

Gene	Function	Fold change (log_2)	*P* value
Rv2913c	*N*-Acyl-D-glutamate amidohydrolase	−2.1	0.00005
Rv0792c	FAD-dependent NAD(P)-disulfide oxidoreductase	−1.9	0.00005
Rv2912c	Transcriptional regulator; TetR family	−1.8	0.00005
Rv0791c	N_5,N_{10}-Methylene tetrahydromethanopterin reductase	−1.8	0.00005
Rv2009	Hypothetical protein	−1.6	0.00005
Rv2466c	Hypothetical protein	−1.6	0.00005
Rv0654	Lignostilbene-α,β-dioxygenase	−1.5	0.00005
Rv1807	PPE family protein	−1.4	0.00005
Rv3252c	Alkane-1 monooxygenase	−1.4	0.00005
Rv3463	N_5,N_{10}-methylene tetrahydromethanopterin reductase	−1.4	0.00005
Rv1285	Sulfate adenylyltransferase subunit 2	−1.3	0.00005
Rv1808	PPE family protein	−1.3	0.00005
Rv0768	Aldehyde dehydrogenase	−1.3	0.00005
Rv1168c	PPE family protein	−1.2	0.00005
Rv3054c	NADPH-quinone oxidoreductase	−1.2	0.00005
Rv0251c	Heat shock protein Hsp	−1.1	0.00005
Rv0331	Oxidoreductase (flavoprotein)	−1.1	0.00005
Rv1169c	PE family of proteins	−1.1	0.00005
Rv0105c	LSU ribosomal protein L28p	−1.1	0.00002
Rv2010	Toxin 1; PIN domain	−1.1	0.00005
Rv3174	Putative oxidoreductase	−1.1	0.00160
Rv3615c	RD1-dependent secreted antigen	−1.1	0.00005
Rv1130	2-Methylcitrate dehydratase	−1.1	0.00005
Rv1554	Fumarate reductase subunit C	−1.0	0.00165
Rv0384c	ClpB protein	−1.0	0.00005
Rv2025c	Cobalt-zinc-cadmium resistance protein	−1.0	0.00005
Rv1286	Sulfate adenylyltransferase subunit 1	−1.0	0.00035
Rv1805c	Hypothetical protein	−1.0	0.00005
Rv3614c	ESX-1 secretion system protein	−1.0	0.00005
Rv1552	Succinate dehydrogenase flavoprotein subunit	−1.0	0.00005
Rv3616c	ESX-1 secretion system protein	−1.0	0.00005
Rv1809	PPE family protein	−1.0	0.00005
Rv1639c	Hypothetical protein	−1.0	0.00005
Rv3824c	Polyketide synthase-associated protein PapA1	−1.0	0.00005
Rv3171c	Nonheme haloperoxidase Hpx	−1.0	0.00005
Rv2006	Uncharacterized glycosyl hydrolase	1.0	0.00005
Rv1757c	Mobile element protein	1.0	0.00040
Rv3000	YbbM seven-transmembrane-helix protein	1.0	0.00005
	Hypothetical protein	1.1	0.00005
Rv1370c	Mobile element protein	1.1	0.00055
Rv2815c	Mobile element protein	1.1	0.00010
Rv0342	Isoniazid-inducible protein IniA	1.1	0.00005
	Hypothetical protein	1.1	0.00005
Rv1955	Hypothetical protein	1.2	0.00005
Rv2835c	Glycerol-3-phosphate ABC transporter UgpA	1.3	0.00005
Rv3862c	Transcriptional regulator WhiB-like WhiB6	1.3	0.00010
Rv2450c	Putative saccharopine dehydrogenase	1.3	0.00005
Rv2816c	CRISPR-associated protein Cas2	1.5	0.00005
Rv0341	Isoniazid-inducible protein IniB	1.8	0.00005
Rv2836c	Putative DNA damage-inducible protein F	2.4	0.00005
Rv2817c	CRISPR-associated protein Cas1	3.2	0.00005
	Hypothetical protein	3.7	0.00005
	Hypothetical protein	4.9	0.00005
Rv2819c	CRISPR-associated protein; Csm5 family	5.0	0.00005
Rv2818c	CRISPR-associated protein Csm6	5.3	0.00005
Rv2822c	CRISPR-associated protein; Csm2 family	5.5	0.00005
Rv2823c	CRISPR-associated protein; Csm1 family	5.5	0.00005
Rv2820c	CRISPR-associated RAMP protein; Csm4 family	5.5	0.00005
Rv2824c	CRISPR-associated protein Cas6	5.6	0.00005
Rv2821c	CRISPR-associated RAMP Csm3	5.7	0.00005
	Hypothetical protein	5.8	0.00005

[a]Genes listed without gene names were not annotated in the *M. tuberculosis* H37Rv genome reported by Cole et al. (25). The mean fold change and the *P* value of each gene were directly exported from the analysis with RNA-Rocket.

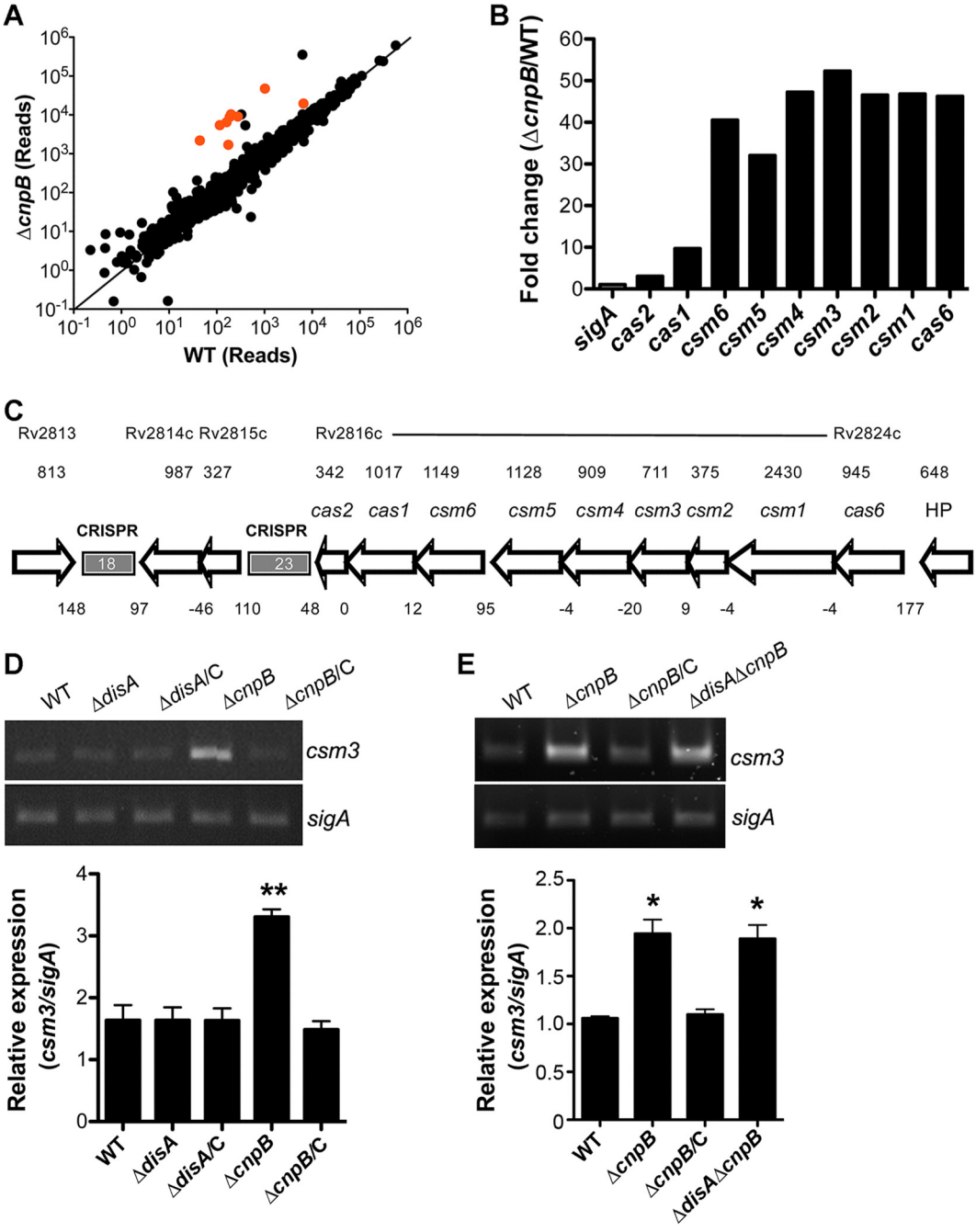

FIG 1 Expression controlled by CnpB in *M. tuberculosis*. (A) RNA reads of all the genes in WT and Δ*cnpB* strains determined using RNA-Seq were plotted. The *cas* genes are indicated in red. The data plotted are the means of three biological repeats analyzed using RNA-Rocket. (B) RNA fold changes of the *cas* genes in *M. tuberculosis* Δ*cnpB* compared to those in the WT determined using RNA-Seq. The data shown are the means analyzed from three biological repeats ($P = 5 \times 10^{-5}$ for all the *cas* genes). (C) Genetic organization of the CRISPR-Cas system in *M. tuberculosis*. The size of each gene (in base pairs) is indicated above the gene. The size of each intergenic region (in base pairs) is also indicated between the related adjacent genes. Negative numbers indicate overlaps between the adjacent genes. (D) Results of RT-PCR of *csm3* in *M. tuberculosis* WT, Δ*disA*, and Δ*cnpB* strains and the complemented mutants (Δ*disA* Δ*disC* and Δ*cnpB* Δ*cnpC*). (E) Results of RT-PCR of *csm3* in BCG WT, Δ*cnpB*, complemented Δ*cnpB* (Δ*cnpB* Δ*cnpC*), and Δ*disA* Δ*cnpB* strains. (D and E) The gel images shown are representative of three repeat experiments. The PCRs of *sigA* served as controls for normalization of the cDNAs. The relative expression of *csm3* versus that of *sigA* was quantitated using ImageJ. The bar graphs show the means of three independent experiments. The error bars indicate the standard errors of the means (SEM). Note that the *M. tuberculosis* Δ*disA* Δ*cnpB* strain exhibited a result similar to that for the double mutant of BCG, and therefore, the result for the *M. tuberculosis* double mutant is not shown. *, $P < 0.05$; **, $P < 0.01$ compared to the WT.

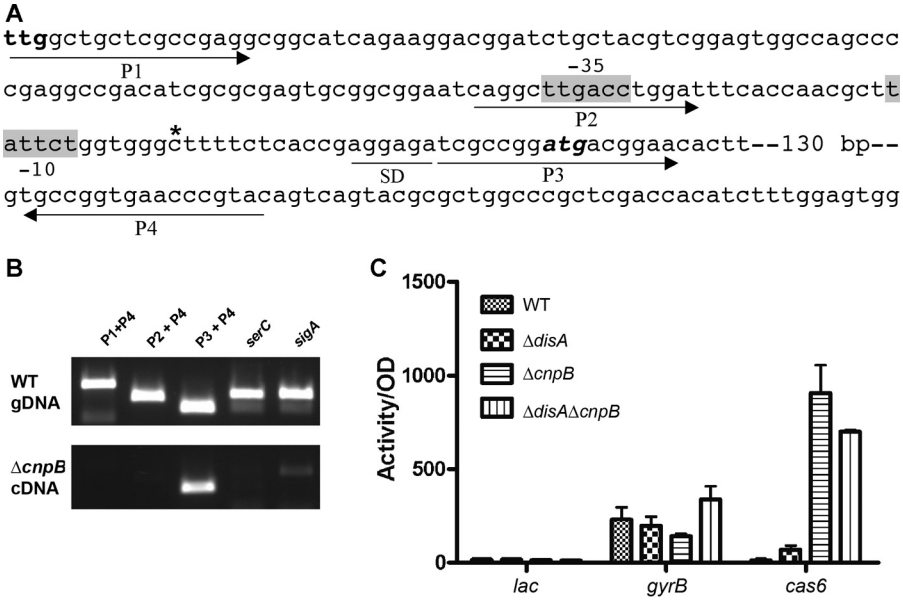

FIG 2 Transcriptional analysis of *cas6*. (A) DNA sequence upstream of *cas6*. **ttg**, annotated start codon of *cas6*; **atg**, start codon of *cas6* that we predicted. Putative −10, −35, and SD sequences are marked. The transcription start site mapped using 5′-RACE is indicated by the asterisk. The primers (P1 to P4) used for the RT-PCRs in panel B are also indicated. (B) RT-PCR analysis of *cas6* transcripts using the primers indicated in panel A. *sigA* was used as a positive control. *serC* represents RT-PCR with primers flanking an intergenic region between *serC* and Rv0885, which served as a negative control without transcript. The data shown are a representative of three repeat experiments. (C) β-Galactosidase assays of BCG WT, Δ*disA*, Δ*cnpB*, and Δ*disA* Δ*cnpB* harboring the vector control (*lacZ*) or promoter fusions for *gyrB* and *cas6*. The promoter fusion with *cas6* was constructed based on our sequence analysis results. Bacteria were grown 7 days prior to the assays. *lac*, a promoterless control; *gyrB*, a constitutive expression control; *cas6*, *lacZ* fused with the *cas6* promoter. The data shown are the means of three repeat experiments. The error bars indicate SEM.

tuberculosis CRISPR-Cas system consists of two CRISPR arrays and nine *cas* genes in the locus (16, 17) (Fig. 1C). We used *csm3* as a representative to validate the RNA-Seq results by reverse transcription (RT)-PCR. The results showed that *csm3* expression was significantly elevated in the Δ*cnpB* strain, which is consistent with the RNA-Seq data. The expression of *csm3* in the Δ*cnpB* strain was reduced to the WT level by complementation of the mutant with *cnpB* (Fig. 1D), indicating that the altered expression of the CRISPR-Cas system is CnpB specific. A similar result was also observed with the BCG strains (Fig. 1E). Surprisingly, the expression of *csm3* was not altered by deletion of *disA*, which encodes the c-di-AMP synthase, in both the WT and Δ*cnpB* genetic backgrounds (Fig. 1D and E), indicating that the regulation of the CRISPR-Cas systems of *M. tuberculosis* and BCG by CnpB is independent of c-di-AMP.

Determination of the transcription start site of the *cas* operon. In order to characterize the expression of the *cas* genes, we cloned a 197-bp DNA fragment upstream of the *cas6* open reading frame (ORF) into a promoterless *lacZ* reporter plasmid based on the annotation of the *M. tuberculosis* genome (25) and transformed this *cas6-lacZ* reporter plasmid into BCG WT and Δ*cnpB* strains. Neither engineered strain exhibited β-galactosidase activity (data not shown), which is inconsistent with the RNA-Seq results. We noticed putative −35 (TTGACC), −10 (TATTCT), and Shine-Dalgarno (SD) (AGGAGA) sequences downstream of the annotated translation start codon (Fig. 2A). Therefore, we hypothesized that the translation start codon for *cas6* was misannotated and the actual translation started 156 bp downstream from the site annotated (Fig. 2A). To verify our prediction, we first performed RT-PCRs using three different forward primers (P1 to P3) and one reverse primer (P4), as indicated in Fig. 2A. The results showed that only P3 and P4 amplified a fragment from the cDNA, whereas no amplicon was detected using either P1 or P2 as a forward primer (Fig. 2B). This observation indicates that the transcript of *cas6* is much shorter at the 5′ end than

annotated, which is consistent with our prediction. We further examined the transcription start site of *cas6* by using 5′ rapid amplification of cDNA ends (RACE), which was detected 131 nucleotides (nt) downstream from the annotated translational start codon (Fig. 2A). Based on these analyses, we constructed another *cas6-lacZ* reporter fusion, which exhibited low expression in BCG WT and the Δ*disA* strain but robust expression in the Δ*cnpB* and Δ*disA* Δ*cnpB* strains compared to the *gyrB-lacZ* reporter control (Fig. 2C). This observation is consistent with the results of RT-PCR, the transcription start site mapping, and the RNA-Seq analysis. Therefore, CnpB controls the transcription of the CRISPR-Cas systems of TB complex mycobacteria.

The upregulation of the *cas* genes in the Δ*cnpB* strain is caused by the loss of an Orn-like activity of CnpB. We previously reported that CnpB is capable of hydrolyzing c-di-AMP into AMP (19). However, our new findings clearly indicate that the regulation of the *cas* genes by CnpB is not mediated by c-di-AMP (Fig. 1). It has been reported that CnpB can also cleave c-di-GMP (24) and nanoRNA (23). Therefore, we determined whether the regulation of the *cas* genes by CnpB is mediated by c-di-GMP or nanoRNA.

It has been shown that Rv1357c encodes a c-di-GMP phosphodiesterase (26). We constructed a ΔRv1357c mutant in *M. tuberculosis* and determined the expression of *csm3* in ΔRv1357c by RT-PCR. The results showed that *csm3* expression was not altered by deletion of Rv1357c in *M. tuberculosis* (Fig. 3A), indicating that the regulation of the *cas* operon is not mediated by c-di-GMP.

E. coli Orn is an oligoribonuclease that cleaves 2-mer to 5-mer nanoRNAs. CnpB is a homolog of Orn in terms of nanoRNA cleavage (23). We constructed a plasmid that overexpresses *E. coli orn* and transformed this recombinant plasmid and the control vector, respectively, into *M. tuberculosis* Δ*cnpB*. RT-PCR with these strains showed that the upregulation of *csm3* in Δ*cnpB* was corrected by expressing *orn* but not by the transformation of the control vector (Fig. 3A). Furthermore, we transformed the *orn*-expressing and control plasmids individually into BCG Δ*cnpB*, which harbors the *cas6-lacZ* reporter fusion. As a result, the high activity of β-galactosidase in the Δ*cnpB* strain was dramatically reduced by the expression of *orn* but not by the transformation of the control vector (Fig. 3B). These results indicate that CnpB controls the expression of the *cas* genes by an activity similar to that of *E. coli* Orn.

To exclude the possibility that Orn also cleaves c-di-AMP, we determined bacterial c-di-AMP levels in an *M. tuberculosis* WT strain and Δ*cnpB* strains harboring the *orn*-expressing plasmid or the empty vector as a control. As expected, expression of *orn* did not significantly reduce the c-di-AMP levels of Δ*cnpB* compared to the levels in a Δ*cnpB* strain bearing the empty vector (Fig. 3C). Furthermore, we purified the Orn protein overexpressed in a recombinant *E. coli* strain and incubated the protein with c-di-AMP, c-di-GMP, or phosphoadenylyl adenosine (pApA) as a 2-mer nanoRNA. The catalytic products were then separated by high-performance liquid chromatography (HPLC). The results showed that Orn cleaved pApA into AMP similarly to CnpB but did not hydrolyze either c-di-AMP or c-di-GMP, which differs from CnpB (Fig. 4; see Fig. S1 in the supplemental material). Since the common function between CnpB and Orn is cleavage of nanoRNA, we conclude that CnpB controls the expression of the *cas* genes in TB complex mycobacteria through an Orn-like activity, which is very likely mediated by nanoRNA.

CnpB controls the levels of crRNAs in TB complex mycobacteria. It has been reported that the *M. tuberculosis* CRISPR-Cas system consists of two CRISPR arrays and nine *cas* genes in the locus (16, 27). However, whether mycobacteria are able to process CRISPR RNA (crRNA) and how the crRNA levels are controlled are unexplored. Our RNA-Seq data showed much higher reads for not only the *cas* genes but also the CRISPR arrays in the Δ*cnpB* strain than in the WT (Fig. 1A and 5). We explored whether precursor crRNA (pre-crRNA) or processed crRNA is upregulated by deletion of *cnpB*. Since *M. tuberculosis* and BCG possess similar CRISPR-Cas systems, except that the numbers of repeats vary between the two strains, we used BCG as a surrogate for

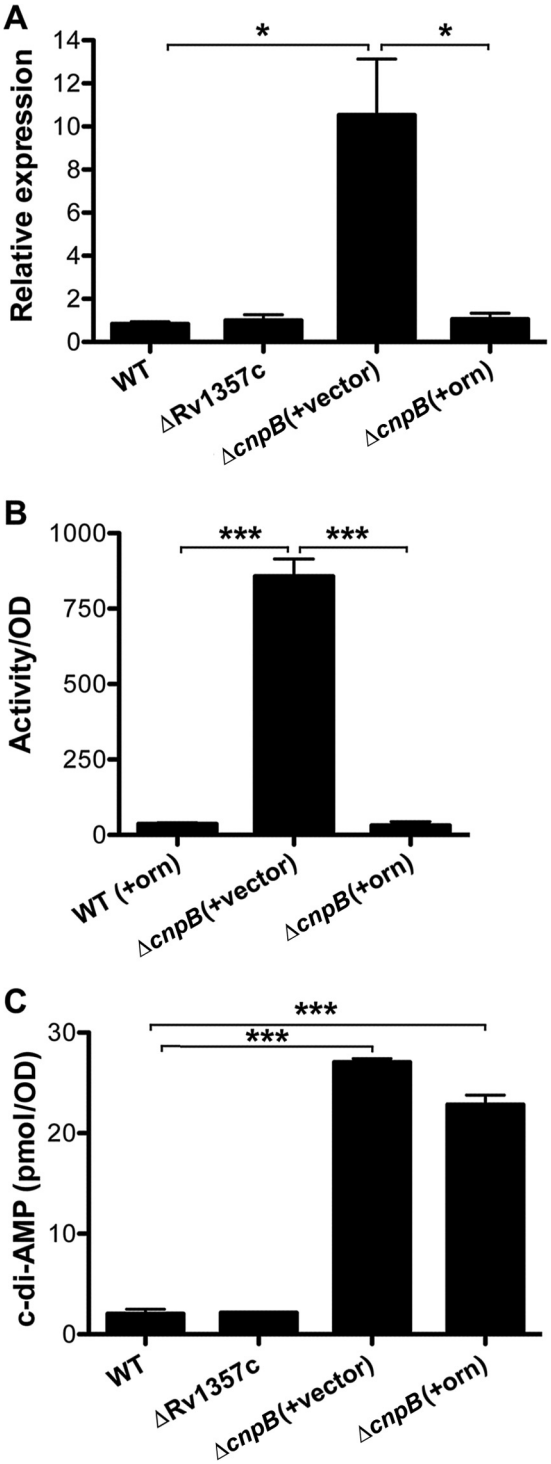

FIG 3 Regulation of the *cas* genes by CnpB. (A) Results of RT-PCR of *csm3* in *M. tuberculosis* WT, ΔRv1357c, Δ*cnpB* expressing *orn* (+*orn*), and Δ*cnpB* harboring the control vector (+vector) strains. The PCR bands were quantitatively analyzed using ImageJ. The relative expression of *csm3* was normalized by that of *sigA*. (B) β-Galactosidase assays of *cas6* promoter-reporter fusion in *orn*-expressing (+*orn*) BCG WT and Δ*cnpB* strains. The BCG Δ*cnpB* strain bearing an expression vector (+vector) was used as a control. The *cas6* promoter fusion was constructed based on our mapping results. Note that the expression of the promoter fusion in BCG WT harboring the vector control was indistinguishable from that in the WT expressing *orn*, and therefore, it is not shown. (C) Determination of intrabacterial c-di-AMP levels in *M. tuberculosis* WT, ΔRv1357c, Δ*cnpB* expressing *orn* (+*orn*), and Δ*cnpB* harboring the control vector (+vector) strains. Samples were prepared from 7-day cultures and analyzed using ELISA. The data shown are the means of three repeat experiments. The error bars indicate SEM. *, $P < 0.05$; ***, $P < 0.001$.

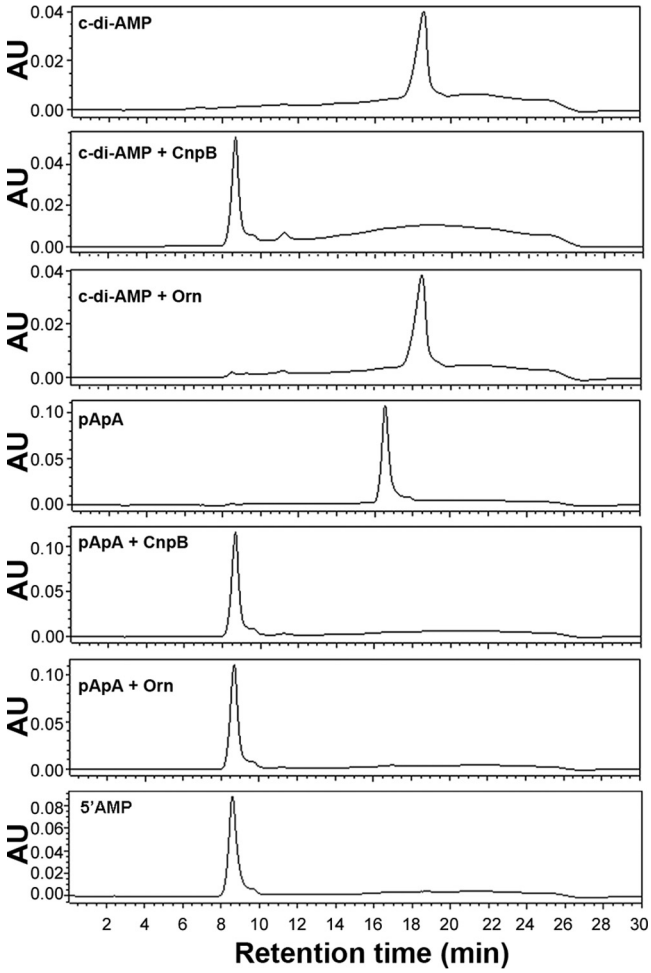

FIG 4 Enzymatic activities of CnpB and Orn determined using HPLC. Purified proteins were incubated with c-di-AMP or pApA. Purified c-di-AMP and pApA were individually analyzed as standards. AU, absorbance units.

M. tuberculosis to determine the RNA levels. We first compared pre-crRNA levels in the WT and Δ*cnpB* strains. The results showed that pre-crRNAs were upregulated in the Δ*cnpB* strain, which was corrected by the complementation of the mutant with *cnpB* (Fig. 6).

The size of the repeat sequence within the CRISPR arrays of both *M. tuberculosis* and BCG is 36 bp. The spacers in the *M. tuberculosis* CRISPR arrays are 25 to 41 bp, whereas they are 25 to 43 bp in BCG. Therefore, most of the processed crRNAs in BCG should be smaller than 70 nt. By using Northern blotting with a probe specific to the repeat sequence, we detected multiple RNA bands with sizes mostly smaller than that of the 73-nt His-tRNA control (Fig. 7). This result indicates that the CRISPR-Cas system in BCG is capable of processing pre-crRNAs into crRNAs. We also found levels of crRNAs in the Δ*cnpB* strain higher than those in the WT, which could be reduced by the complementation of the mutant with *cnpB* (Fig. 7; see Fig. S2 in the supplemental material). As expected, deletion of *disA* in the Δ*cnpB* genetic background did not alter the levels of crRNAs, indicating that the control of crRNAs by CnpB is c-di-AMP independent (Fig. 7). Interestingly, the elevated crRNA levels in the Δ*cnpB* strain were partially reduced by the expression of *E. coli orn* but not by the transformation of the control vector (Fig. 7), suggesting that the upregulation of the crRNAs by the deletion of *cnpB* is mediated by the loss of an Orn-like activity of CnpB. Taking the data together, we conclude that CnpB controls crRNA levels through an Orn-like activity, which is very likely mediated by nanoRNA, in TB complex mycobacteria.

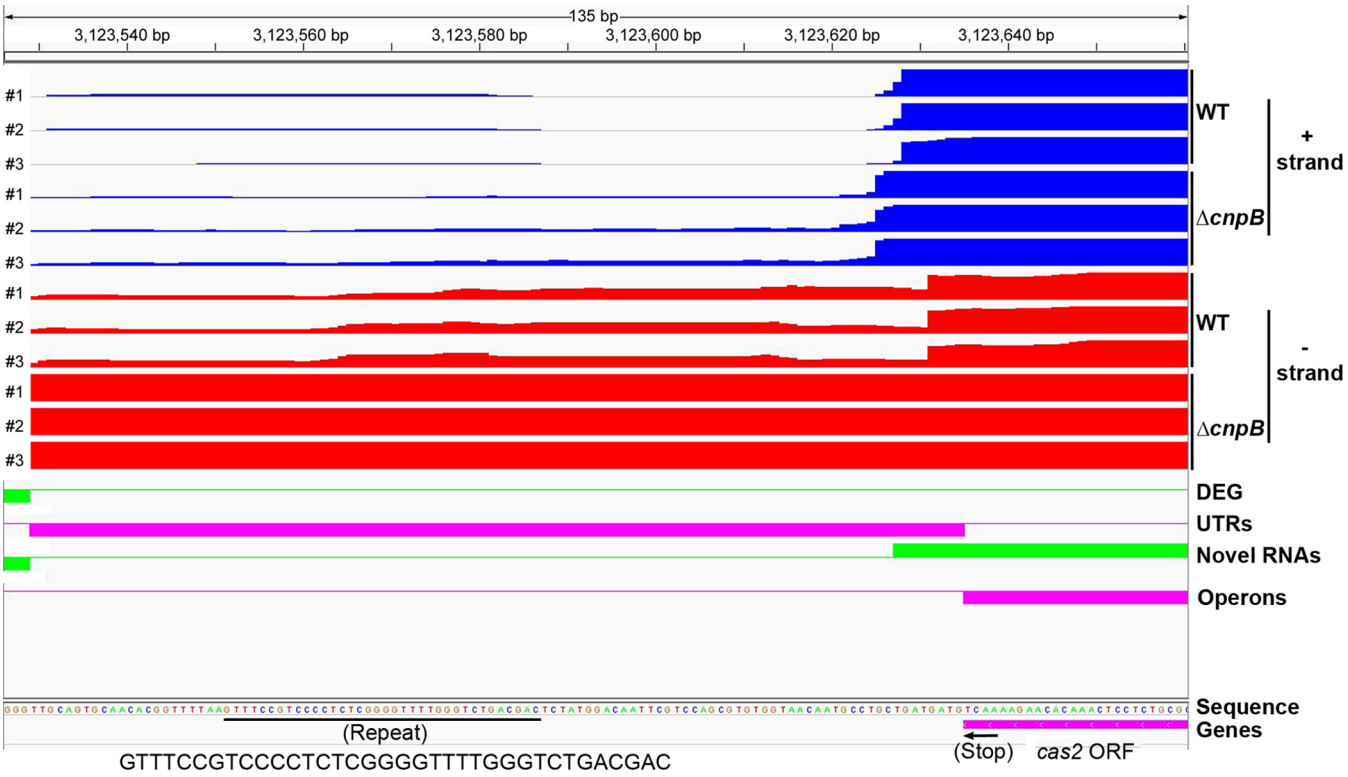

FIG 5 Comparison of reads of *cas2* and its downstream RNA of *M. tuberculosis* WT and Δ*cnpB* analyzed using the Rockhopper program. Expression from both the positive strand (blue) and the negative strand (red) of the WT and Δ*cnpB* strains, respectively, is shown. The translational stop codon of *cas2* is indicated with an arrow. The sequence of the first repeat in the complement orientation is indicated. DEG, differentially expressed genes; operons, multigene operons; UTRs, untranslated regions.

DISCUSSION

The CRISPR-Cas systems in TB complex mycobacteria have been recognized based on sequence analyses (16, 17) but have not been investigated experimentally. DHH superfamily proteins include RecJ, nanoRNases (NrnA), c-di-AMP phosphodiesterases, and pyrophosphatases (28). According to our current knowledge, *M. tuberculosis* CnpB is a DHH superfamily protein that cleaves c-di-AMP, c-di-GMP, and nanoRNA (19, 23). In this study, we found that CnpB controls the CRISPR-Cas systems in TB complex mycobacteria mediated by an Orn-like activity, possibly through nanoRNA rather than

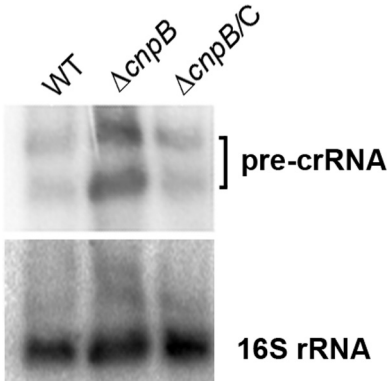

FIG 6 Northern blot analysis of pre-crRNAs. RNA samples of BCG WT, Δ*cnpB*, and complemented mutant strains were separated on 1% denatured agarose gels. After transfer onto a Hybond membrane, they were first hybridized with a probe specific to the *M. tuberculosis* CRISPR repeat sequence. The membrane was then stripped and reprobed with an oligonucleotide specific to *M. tuberculosis* 16S rRNA. The data shown are representative of three repeat experiments.

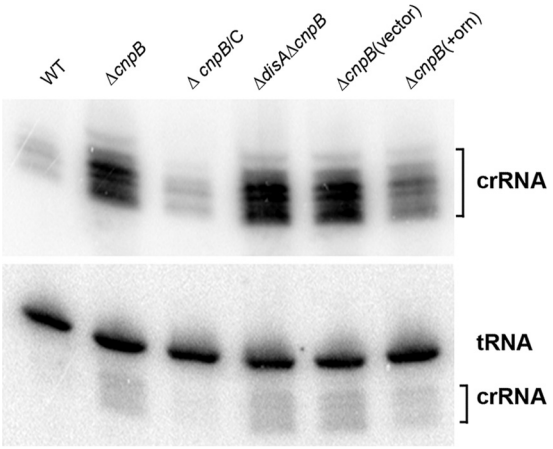

FIG 7 Northern blot analysis of crRNAs. RNA samples of BCG WT, Δ*cnpB*, complemented Δ*cnpB*, Δ*disA* Δ*cnpB*, Δ*cnpB* expressing *orn*, and Δ*cnpB* bearing the control vector were separated in 10% polyacrylamide gels. After transfer onto a Hybond membrane, they were first hybridized with a probe specific to the *M. tuberculosis* CRISPR repeat sequence. The membrane was then stripped and reprobed with an oligonucleotide specific to *M. tuberculosis* His-tRNA. Note that the crRNA probes were not fully stripped off and residual signals remained in the blot with His-tRNA. The data shown are representative of three repeat experiments.

c-di-AMP or c-di-GMP (Fig. 8). Our study also shows for the first time that TB complex mycobacteria encode a functional system to process crRNAs.

The components of CRISPR-Cas systems in some bacteria and their roles in gene editing have been well recognized. In contrast, our knowledge about regulation of CRISPR-Cas systems is still in an early stage. In several bacterial species, it has been shown that CRISPR-Cas systems are transcriptionally regulated by transcription factors, such as CRP, H-NS, LRP, and LeuO (9–15). In addition to these pleiotropic or global regulators, some dedicated regulators have also been shown to control the expression of CRISPR-Cas systems. These regulators include DevS of *Myxococcus xanthus* and Csa3 proteins of *Sulfolobus islandicus* (29).

The role of nanoRNAs in regulation of a CRISPR-Cas system has not been reported. It is possible that the regulation of the CRISPR-Cas system by CnpB that we found is orchestrated by a nanoRNA-responsive transcription factor. A CRP homolog (Rv3676) in *M. tuberculosis* has been well studied, but this transcription factor does not regulate the CRISPR-Cas system, according to multiple global gene expression analyses of *M.*

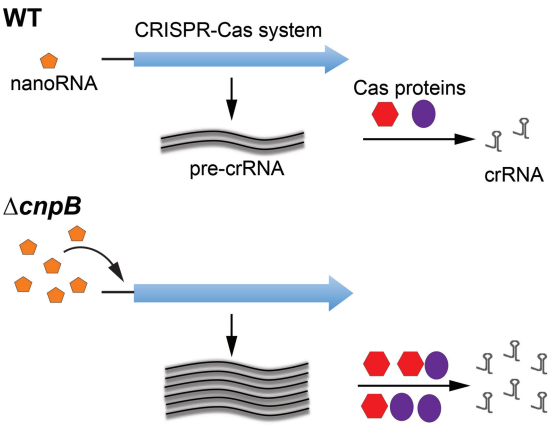

FIG 8 Hypothetical model of CnpB-controlled CRISPR-Cas system in TB complex mycobacteria. The meanings of the symbols in the Δ*cnpB* strain diagram are identical to those in the WT diagram. In this model, more nanoRNAs were accumulated in the Δ*cnpB* strain than in the WT, which induces the expression of both pre-crRNA and the *cas* genes. Eventually, more crRNAs were generated in the Δ*cnpB* strain than in the WT.

tuberculosis Δ*crp* (30–32). Homologs of LRP (Rv3291c and Rv2779c) (33–36) and H-NS (Rv3597c) (37–40) have also been characterized in *M. tuberculosis*. However, it is unknown whether these homologs or other dedicated regulators regulate the expression of the *cas* genes, which warrants further investigation.

RNA turnover is an essential bioprocess in all organisms and is associated with the regulation of gene expression. RNA is degraded by RNases, but some RNases are unable to completely cleave the target RNAs. NanoRNAs are RNA degradation products of these RNases. For example, the end products of degradation catalyzed by RNase II and RNase R range from 1-mers to 6-mers, which vary in size with different RNases (41). *M. tuberculosis* CnpB and its homolog in *Mycobacterium smegmatis* have been shown to cleave 2-mer nanoRNAs (28). This process likely provides a source for nucleotide recycling. Bacterial nanoRNA levels in this study were not reported, as we had technical difficulty in examining nanoRNA by following a method used for *Pseudomonas aeruginosa* (42). Interestingly, in an *orn* deletion mutant of *P. aeruginosa*, nanoRNAs of 2-mers to 4-mers accumulate within bacteria and prime transcription initiation, which results in widespread transcription start site shifting (42). Additionally, the use of nanoRNAs to prime transcription initiation is also coupled with global alterations in gene expression, with a total of 1,158 genes differentially expressed in the *orn* mutant (42). Transcription start site shifting of *cas6* is possible based on the assembled RNA reads. However, it is surprising that many fewer genes are differentially expressed in *M. tuberculosis* Δ*cnpB* than in the Δ*orn* mutant of *P. aeruginosa*. Only the genes in the *cas* operon are highly expressed in *M. tuberculosis* Δ*cnpB*, suggesting that the upregulation of these genes is not due to transcription start site shifting caused by nanoRNA. The molecular basis of the CnpB-mediated gene regulation of *M. tuberculosis* will be further explored in our future studies.

crRNA is assembled into a ribonucleoprotein complex with Cas proteins. Six types of CRISPR-Cas systems are grouped into two classes: class 1 comprises multisubunit effector complexes, whereas class 2 possesses a single complex (6–8). Based on sequence analysis of the Cas proteins, *M. tuberculosis* possesses a class 1 type III CRISPR-Cas system (5). This type of CRISPR-Cas system typically targets single-stranded RNA (ssRNA) in a protospacer-adjacent motif (PAM)-independent manner (8). The target RNA-bound complex cleaves the target RNA transcript and, in addition, has a target RNA-stimulated nonspecific DNase activity that cleaves single-stranded DNA (8, 43–45). How the *M. tuberculosis* CRISPR-Cas system cleaves nucleic acids remains to be investigated.

The repeat sequences in the CRISPR arrays of TB complex mycobacteria are highly conserved, whereas the spacers vary slightly among different species (16). It is known that bacteria acquire spacer sequences from prior invasion of bacteriophages or plasmids. We compared all the *M. tuberculosis* spacer sequences with the Actinobacteriophage Database (http://www.phagesdb.org), which includes 1,435 currently sequenced mycobacteriophages. None of the spacer sequences matched any mycobacteriophage sequence. As pointed out by He et al., nearly all mycobacteriophages were initially isolated using *M. smegmatis*, in which no CRISPR locus can be found, as a host (16). Therefore, the targets of crRNAs of TB complex mycobacteria remain completely unknown, and exploration of these targets will provide more insights into the understanding of mycobacterial biology.

MATERIALS AND METHODS

Bacterial strains and growth conditions. *M. tuberculosis* H37Rv and BCG (strain Pasteur [Trudeau Institute]) and their derivatives were used in this study. Δ*disA*, Δ*cnpB*, and Δ*disA* Δ*cnpB* mutants of both *M. tuberculosis* and BCG were reported previously (19, 20). Both the Δ*disA* and Δ*cnpB* mutants were complemented as described previously (19, 20). Bacteria were grown in mycomedium (Middlebrook 7H9 medium [BD] supplemented with 0.5% glycerol, 10% oleic acid-albumin-dextrose-catalase [OADC], and 0.05% Tween 80), Sauton's medium (46), or Middlebrook 7H10 agar (BD) supplemented with 10% OADC and 0.01% cycloheximide. Fresh cultures were inoculated from frozen stocks for every experiment. Bacteria were grown in tissue culture flasks standing with ambient air unless otherwise specified. *E. coli* strains were grown in Luria-Bertani (LB) broth or on LB agar plates. *M. smegmatis* mc^2155 was grown in mycomedium. All cultures were grown at 37°C, except *M. smegmatis*, which was grown at 30°C in

TABLE 2 Plasmids used in this study

Plasmid	Description[a]	Source or reference
pJSC407	*M. tuberculosis* knockout plasmid; Hyg^r	47
phAE159	Knockout phasmid; Carb^r	48
pGB003	pJSC407 carrying Rv1357c upstream fragment; Hyg^r	This study
pGB004	pGB003 carrying Rv1357c downstream fragment; Hyg^r	This study
pGB005	phAE159 carrying pGB004 plasmid DNA; Hyg^r	This study
pMBC1260	pMBC304 carrying Rv0805 promoter; Kan^r Ap^r	19
pGB228	pMBC1260 carrying *E. coli orn* ORF; Kan^r Ap^r	This study
pET28a(+)	Expression plasmid; Kan^r	Novagen
pGB282	pET28a(+) carrying *E. coli orn* ORF; Kan^r	This study
pLACint	Promoter reporter vector with a promoterless *lacZ*; Kan^r	56
pGB232	pLacint carrying putative *cas6* promoter (annotated); Kan^r	This study
pGB248	pLacint carrying putative *cas6* promoter (identified); Kan^r	This study

[a]Hyg^r, hygromycin resistance; Kan^r, kanamycin resistance; Carb^r, carbenicillin resistance; Ap^r, ampicillin resistance.

mycomedium. Kanamycin at 25 μg/ml, hygromycin at 50 μg/ml, or zeocin at 100 μg/ml was added when necessary.

Deletion of Rv1357c in *M. tuberculosis*. All the plasmids used in this study are listed in Table 2. To construct strain ΔRv1357c of *M. tuberculosis*, an upstream fragment was amplified by PCR with primers JY007 and JY008 (see Table S1 in the supplemental material). This fragment was first cloned using a TA cloning kit (Invitrogen) and then subcloned into pJSC407 (kindly provided by Jeffery Cox [47]) between EcoRV and HindIII sites to generate pGB003. A downstream fragment of Rv1357c was amplified by PCR with primers JY009 and JY010 (see Table S1 in the supplemental material). The fragment was first cloned using the TA cloning kit (Invitrogen) and then subcloned into pGB003 between XbaI and KpnI sites to generate pGB004. Plasmid pGB004 was digested with PacI, ligated with PacI-digested phasmid phAE159 (generously provided by William Jacobs, Jr.) overnight, and then packaged using MaxPlax lambda packaging extracts (Epicentre Biotechnoloies) to generate phasmid pGB005 in *E. coli* HB101. The recombinant phasmid DNA was prepared from hygromycin-resistant colonies and transformed into *M. smegmatis* mc^{2}155. Phages were prepared from a plaque derived from *M. smegmatis* by a method similar to that in previous reports (48, 49). *M. tuberculosis* bacteria grown to log phase were infected with high-titer phages. Hygromycin-resistant ΔRv1357c candidates were further screened by PCR using primers listed in Table S1 in the supplemental material.

RNA extraction. Total-RNA extraction from bacteria was carried out using the method reported by Mangan et al. (50). For RNA-Seq analysis and RT-PCR, the total RNA was treated twice with RNase-free DNase I on column with an RNeasy minikit (Qiagen) and an RNase-Free DNase set (Qiagen) following the manufacturer's instructions. For Northern blotting, RNA was treated twice with RNase-free DNase I in solution. The RNA concentration was determined spectrophotometrically using a Biophotometer (Eppendorf) at 260 nm. PCR of *sigA* was performed, using 0.1 μg of total RNA as a template, to ensure the absence of DNA contamination in the RNA samples.

RNA-Seq analysis. For RNA-Seq analysis, RNA samples for three biological experiments were prepared. rRNA was removed from 2.5 μg of each total-RNA sample using the Ribo-Zero magnetic kit (Epicentre). Strand-specific DNA libraries for Illumina sequencing were prepared using the ScriptSeq complete kit (Epicentre) following the manufacturer's manual. Sequencing was performed using an Illumina HiSeq instrument at the University at Buffalo Next Generation Sequencing and Expression Analysis Core Facility. Sequencing files were uploaded to Galaxy of RNA-Rocket (http://rnaseq.pathogenportal.org), trimmed, aligned, and assembled according to the annotation of *M. tuberculosis* H37Rv (25). To compare RNA reads, RNA-Seq data were also uploaded to Rockhopper (https://cs.wellesley.edu/~btjaden/Rockhopper/) and analyzed using the program (51, 52).

Synthesis of cDNA and RT-PCR. cDNA was prepared and amplified as previously described (53). Control reactions were performed using primers specific to 16S rRNA (54) or *sigA* (55) (see Table S1 in the supplemental material). PCR products were separated on 2% agarose gels. The mean intensity of each band was analyzed using ImageJ software (National Institutes of Health [NIH]). The relative expression was calculated by normalizing the intensity of the *csm3* band with that of the *sigA* band amplified with the same cDNA sample.

Cloning of promoters. The annotated intergenic region between Rv2824c and Rv2825c was PCR amplified using primers JY392 and JY393 (see Table S1 in the supplemental material). The promoter region that we predicted was amplified using primers JY432 and JY433. The PCR products were individually cloned into a single-copy integrative vector, pLACint, upstream of a promoterless *lacZ* gene, as previously reported (56).

β-Galactosidase activity assay. Bacteria were grown to exponential phase by shaking at 37°C in mycomedium. A 300-μl portion of each strain was transferred to a fresh tube, followed by sonication as reported previously (57). The β-galactosidase activity was measured by a method similar to that in a previous report (58) using the fluorescent dye 5-acetylamino-fluorescein di-β-D-galactopyranoside (C_2FDG) (Molecular Probes) and read in a CytoFluor multiwell plate reader (PerSpective Biosystems). Activity readings were normalized by the optical density of each culture at 650 nm (OD_{650}), determined

using a Thermomax microplate reader (Molecular Devices). The results were expressed as β-galactosidase activity divided by the OD.

Expression and purification of proteins. Recombinant protein of *M. tuberculosis* CnpB was expressed and purified similarly to what we reported previously (19). The ORF of *E. coli orn* was amplified by PCR using primers JY518 and JY519 (see Table S1 in the supplemental material) and *E. coli* DH5α DNA as the template. The PCR product was digested with NdeI and HindIII and cloned into NdeI-HindIII-digested pET28a(+) (Novagen) to generate pGB282. This plasmid was transformed into *E. coli* BL21(DE3) to express Orn. The recombinant protein was purified by a method similar to what we reported previously (18, 59). Briefly, an overnight culture was inoculated in 500 ml LB broth containing 25 μg/ml kanamycin and incubated at 37°C with shaking to an OD_{600} of 0.6. The culture was then cooled to room temperature, followed by the addition of isopropyl-β-D-1-thiogalactopyranoside (IPTG) to a final concentration of 0.1 mM. After induction at room temperature for 4 h, the bacteria were harvested by centrifugation at 6,000 rpm for 10 min. The bacterial pellet was resuspended in 50 ml of buffer A (50 mM Tris-HCl, 150 mM NaCl, 10 mM imidazole, 10% glycerol) with 1% protease inhibitor (Roche) and sonicated on ice for 10 min, with 5-s pulses and 10-s intervals. After centrifugation at 12,000 rpm for 30 min at 4°C, the supernatant was loaded onto an Ni-nitrilotriacetic acid (NTA)-agarose column preequilibrated with buffer A at a flow rate of 0.5 ml/min. The column was subsequently washed with 50 ml of buffer B (50 mM Tris-HCl, 500 mM NaCl, 20 mM imidazole, pH 7.5) and 50 ml buffer C (50 mM Tris-HCl, 500 mM NaCl, 50 mM imidazole, pH 7.5) at 1 ml/min. The His-tagged proteins were eluted with 10 ml buffer D (50 mM Tris-HCl, 500 mM NaCl, 300 mM imidazole, pH 7.5) at 0.5 ml/min. All the eluted fractions were analyzed by SDS-PAGE, and collections were dialyzed against phosphate-buffered saline (PBS) at 4°C. The purified protein was stored in PBS with 10% glycerol at −80°C until it was used.

Expression of *E. coli orn* in mycobacteria. The *E. coli orn* ORF was amplified by PCR using primers JY388 and JY389 (see Table S1 in the supplemental material) and *E. coli* DH5α DNA as the template. The PCR product was digested with KpnI and cloned into pMBC1260 at the KpnI site to generate pGB228. The inserted DNA was verified by PCR and sequencing. Plasmids pGB228 and, as the control plasmid, pMBC1260 were individually transformed into Δ*cnpB* mutants of *M. tuberculosis* and BCG, respectively, by electroporation. Transformants were selected on Middlebrook 7H10 plates containing 25 μg/ml kanamycin and were further verified by PCR prior to making stocks.

HPLC. The reaction mixtures (10 μl) to determine the activity of Orn contained 50 mM Tris-HCl (pH 7.5), 1 mM $MnCl_2$, and 0.5 mM the indicated nucleotide. The reaction was initiated by adding Orn or CnpB protein to 3 μM and was incubated for 1 h at 37°C. Subsequently, each reaction was terminated by adding 1 μl of 0.5 M EDTA, and the reaction mixture was diluted 1:5 with water. Finally, 20 μl of each sample was injected and separated by reverse-phase HPLC with a C_{18} column (250 by 4.6 mm; Vydac) using a Waters 625 LC system equipped with a 996 photodiode array detector and a 717 autosampler (Waters). The samples were eluted using the same buffers we reported previously (60). Nucleotides were monitored at 254 nm.

Detection of c-di-AMP. Bacteria were grown in mycomedium for 7 days. After determination of the OD_{600} of each strain, the bacteria were harvested, and each bacterial pellet was resuspended in 0.5 ml 50 mM Tris-HCl (pH 8.0), heat killed, and disrupted with 1-mm beads using a bead beater (BioSpec). The lysate was collected, and the bacterial debris was removed by centrifugation for 10 min at 13,000 rpm. The supernatant was used as a bacterial c-di-AMP sample. c-di-AMP was then detected using an enzyme-linked immunosorbent assay (ELISA) as we described previously (61–63).

RACE. The transcription start site was determined using 5′ RACE by following a previously reported method (64). Briefly, 5 μg total RNA of WT BCG was reverse transcribed using a *cas6*-specific primer, JY534 (see Table S1 in the supplemental material). cDNA was treated with an RNase H and RNase T1 mixture at 37°C for 30 min and was then purified with a S.N.A.P column (Invitrogen). A poly(C) tail was added to the cDNA at the 5′ end using terminal deoxynucleotidyl transferase (TdT). Subsequently, cDNA was amplified by PCR using primers JY532 and JY535 (see Table S1 in the supplemental material). The PCR product was cloned using a TA cloning kit (Invitrogen). The inserted DNA was sequenced with primer JY535 to determine the 5′ end of the transcript.

Northern blot analysis. Northern blots were used to compare levels of both pre-crRNA and crRNA among different bacterial strains. DNA oligonucleotide probes specific for each RNA (see Table S1 in the supplemental material) were end labeled using 20 pmol of the oligonucleotide in a 10-μl reaction mixture containing 25 μM [γ-^{32}P]ATP (MP Biomedicals) and 20 units T4 polynucleotide kinase (NEB) at 37°C for 1 h.

For Northern blotting of pre-crRNA, 5 μg total RNA was separated on a 1% denaturing formaldehyde agarose gel, which was capillary transferred onto a positively charged membrane (Hybond N+; GE Life Sciences) for blotting. Northern blotting of crRNA was performed by a method similar to that in a previous report (65). Briefly, 5 μg total RNA was separated on a 10% denaturing polyacrylamide gel, which was electronically transferred to a Hybond membrane for blotting. Hybridization was performed using Amersham Rapid-hyb buffer (GE Healthcare), following the recommended protocol for oligonucleotide probes, with a 6-h incubation at 42°C. The blotted membranes were washed once with 2× SSC (1× SSC is 0.15 M NaCl plus 0.015 M sodium citrate) containing 0.1% SDS and twice with 0.2× SSC containing 0.1% SDS. The membranes were exposed to a PhosphorImager screen (Molecular Dynamics), scanned with a Storm 860 scanner (Molecular Dynamics), and analyzed with ImageQuant software (Molecular Dynamics). Subsequently, the hybridized membranes were stripped with a stripping solution (5 mM Tris-HCl, pH 8.0, 0.2 mM EDTA, 0.05% Na-pyrophosphate, 0.1× Denhardt's solution) for 30 min to 3 h at 80°C, followed by hybridization with different probes.

Statistical analysis. All the data were analyzed by a two-tailed *t* test using Prism 5 (GraphPad Software), except that RNA-Seq data were exported from RNA-Rocket analysis. *P* values of <0.05 were considered to be statistically significant.

Accession number(s). The RNA-Seq data have been deposited at NCBI Gene Expression Ominibus (GEO) under accession number GSE102816.

SUPPLEMENTAL MATERIAL

Supplemental material for this article may be found at https://doi.org/10.1128/JB.00743-17.

SUPPLEMENTAL FILE 1, PDF file, 0.4 MB.

ACKNOWLEDGMENTS

We thank Jeffery Cox for providing pJSC407 and pYO11; William Jacobs, Jr., for providing phAE159; Joseph Wade and Jing Wang for assistance with RNA-Seq analysis; and Kathleen McDonough for β-galactosidase activity assay. We are grateful to the Biochemistry Core of the Wadsworth Center for assistance with HPLC analysis and the Next Generation Sequencing Core Facility of the University at Buffalo for RNA-Seq.

This project is partly supported by a Scientist Development Grant from the American Heart Association 12SDG12080067 to G.B.

We have no conflict of interest to declare.

REFERENCES

1. Bhaya D, Davison M, Barrangou R. 2011. CRISPR-Cas systems in bacteria and archaea: versatile small RNAs for adaptive defense and regulation. Annu Rev Genet 45:273–297. https://doi.org/10.1146/annurev-genet-110410-132430.
2. Sorek R, Lawrence CM, Wiedenheft B. 2013. CRISPR-mediated adaptive immune systems in bacteria and archaea. Annu Rev Biochem 82:237–266. https://doi.org/10.1146/annurev-biochem-072911-172315.
3. Westra ER, Buckling A, Fineran PC. 2014. CRISPR-Cas systems: beyond adaptive immunity. Nat Rev Microbiol 12:317–326. https://doi.org/10.1038/nrmicro3241.
4. Haft DH, Selengut J, Mongodin EF, Nelson KE. 2005. A guild of 45 CRISPR-associated (Cas) protein families and multiple CRISPR/Cas subtypes exist in prokaryotic genomes. PLoS Comput Biol 1:e60. https://doi.org/10.1371/journal.pcbi.0010060.
5. Makarova KS, Haft DH, Barrangou R, Brouns SJ, Charpentier E, Horvath P, Moineau S, Mojica FJ, Wolf YI, Yakunin AF, van der Oost J, Koonin EV. 2011. Evolution and classification of the CRISPR-Cas systems. Nat Rev Microbiol 9:467–477. https://doi.org/10.1038/nrmicro2577.
6. Makarova KS, Wolf YI, Alkhnbashi OS, Costa F, Shah SA, Saunders SJ, Barrangou R, Brouns SJ, Charpentier E, Haft DH, Horvath P, Moineau S, Mojica FJ, Terns RM, Terns MP, White MF, Yakunin AF, Garrett RA, van der Oost J, Backofen R, Koonin EV. 2015. An updated evolutionary classification of CRISPR-Cas systems. Nat Rev Microbiol 13:722–736. https://doi.org/10.1038/nrmicro3569.
7. Mohanraju P, Makarova KS, Zetsche B, Zhang F, Koonin EV, van der Oost J. 2016. Diverse evolutionary roots and mechanistic variations of the CRISPR-Cas systems. Science 353:aad5147. https://doi.org/10.1126/science.aad5147.
8. Tamulaitis G, Venclovas C, Siksnys V. 2017. Type III CRISPR-Cas immunity: major differences brushed aside. Trends Microbiol 25:49–61. https://doi.org/10.1016/j.tim.2016.09.012.
9. Agari Y, Sakamoto K, Tamakoshi M, Oshima T, Kuramitsu S, Shinkai A. 2010. Transcription profile of *Thermus thermophilus* CRISPR systems after phage infection. J Mol Biol 395:270–281. https://doi.org/10.1016/j.jmb.2009.10.057.
10. Medina-Aparicio L, Rebollar-Flores JE, Gallego-Hernandez AL, Vazquez A, Olvera L, Gutierrez-Rios RM, Calva E, Hernandez-Lucas I. 2011. The CRISPR/Cas immune system is an operon regulated by LeuO, H-NS, and leucine-responsive regulatory protein in Salmonella enterica serovar Typhi. J Bacteriol 193:2396–2407. https://doi.org/10.1128/JB.01480-10.
11. Patterson AG, Chang JT, Taylor C, Fineran PC. 2015. Regulation of the type I-F CRISPR-Cas system by CRP-cAMP and GalM controls spacer acquisition and interference. Nucleic Acids Res 43:6038–6048. https://doi.org/10.1093/nar/gkv517.
12. Pul U, Wurm R, Arslan Z, Geissen R, Hofmann N, Wagner R. 2010. Identification and characterization of *E. coli* CRISPR-Cas promoters and their silencing by H-NS. Mol Microbiol 75:1495–1512. https://doi.org/10.1111/j.1365-2958.2010.07073.x.
13. Shinkai A, Kira S, Nakagawa N, Kashihara A, Kuramitsu S, Yokoyama S. 2007. Transcription activation mediated by a cyclic AMP receptor protein from *Thermus thermophilus* HB8. J Bacteriol 189:3891–3901. https://doi.org/10.1128/JB.01739-06.
14. Westra ER, Pul U, Heidrich N, Jore MM, Lundgren M, Stratmann T, Wurm R, Raine A, Mescher M, Van Heereveld L, Mastop M, Wagner EG, Schnetz K, Van Der Oost J, Wagner R, Brouns SJ. 2010. H-NS-mediated repression of CRISPR-based immunity in *Escherichia coli* K12 can be relieved by the transcription activator LeuO. Mol Microbiol 77:1380–1393. https://doi.org/10.1111/j.1365-2958.2010.07315.x.
15. Yang CD, Chen YH, Huang HY, Huang HD, Tseng CP. 2014. CRP represses the CRISPR/Cas system in *Escherichia coli*: evidence that endogenous CRISPR spacers impede phage P1 replication. Mol Microbiol 92:1072–1091. https://doi.org/10.1111/mmi.12614.
16. He L, Fan X, Xie J. 2012. Comparative genomic structures of *Mycobacterium* CRISPR-Cas. J Cell Biochem 113:2464–2473. https://doi.org/10.1002/jcb.24121.
17. Supply P, Marceau M, Mangenot S, Roche D, Rouanet C, Khanna V, Majlessi L, Criscuolo A, Tap J, Pawlik A, Fiette L, Orgeur M, Fabre M, Parmentier C, Frigui W, Simeone R, Boritsch EC, Debrie AS, Willery E, Walker D, Quail MA, Ma L, Bouchier C, Salvignol G, Sayes F, Cascioferro A, Seemann T, Barbe V, Locht C, Gutierrez MC, Leclerc C, Bentley SD, Stinear TP, Brisse S, Medigue C, Parkhill J, Cruveiller S, Brosch R. 2013. Genomic analysis of smooth tubercle bacilli provides insights into ancestry and pathoadaptation of *Mycobacterium tuberculosis*. Nat Genet 45:172–179. https://doi.org/10.1038/ng.2517.
18. Bai Y, Yang J, Zhou X, Ding X, Eisele LE, Bai G. 2012. *Mycobacterium tuberculosis* Rv3586 (DacA) is a diadenylate cyclase that converts ATP or ADP into c-di-AMP. PLoS One 7:e35206. https://doi.org/10.1371/journal.pone.0035206.
19. Yang J, Bai Y, Zhang Y, Gabrielle VD, Jin L, Bai G. 2014. Deletion of the cyclic di-AMP phosphodiesterase gene (*cnpB*) in *Mycobacterium tuberculosis* leads to reduced virulence in a mouse model of infection. Mol Microbiol 93:65–79. https://doi.org/10.1111/mmi.12641.
20. Zhang Y, Yang J, Bai G. 31 January 2018. Cyclic di-AMP-mediated interaction between *Mycobacterium tuberculosis* Δ*cnpB* and macrophages implicates a novel strategy for improving BCG vaccination. Pathog Dis https://doi.org/10.1093/femspd/fty008.
21. Dey RJ, Dey B, Zheng Y, Cheung LS, Zhou J, Sayre D, Kumar P, Guo H, Lamichhane G, Sintim HO, Bishai WR. 2017. Inhibition of innate immune cytosolic surveillance by an *M. tuberculosis* phosphodiesterase. Nat Chem Biol 13:210–217. https://doi.org/10.1038/nchembio.2254.

22. Dey B, Dey RJ, Cheung LS, Pokkali S, Guo H, Lee JH, Bishai WR. 2015. A bacterial cyclic dinucleotide activates the cytosolic surveillance pathway and mediates innate resistance to tuberculosis. Nat Med 21:401–406. https://doi.org/10.1038/nm.3813.
23. Postic G, Danchin A, Mechold U. 2012. Characterization of NrnA homologs from *Mycobacterium tuberculosis* and *Mycoplasma pneumoniae*. RNA 18:155–165. https://doi.org/10.1261/rna.029132.111.
24. He Q, Wang F, Liu S, Zhu D, Cong H, Gao F, Li B, Wang H, Lin Z, Liao J, Gu L. 2016. Structural and biochemical insight into the mechanism of Rv2837c from *Mycobacterium tuberculosis* as a c-di-NMP phosphodiesterase. J Biol Chem 291:3668–3681. https://doi.org/10.1074/jbc.M115.699801.
25. Cole ST, Brosch R, Parkhill J, Garnier T, Churcher C, Harris D, Gordon SV, Eiglmeier K, Gas S, Barry CEIII, Tekaia F, Badcock K, Basham D, Brown D, Chillingworth T, Connor R, Davies R, Devlin K, Feltwell T, Gentles S, Hamlin N, Holroyd S, Hornsby T, Jagels K, Krogh A, McLean J, Moule S, Murphy L, Oliver K, Osborne J, Quail MA, Rajandream MA, Rogers J, Rutter S, Seeger K, Skelton J, Squares R, Squares S, Sulston JE, Taylor K, Whitehead S, Barrell BG. 1998. Deciphering the biology of *Mycobacterium tuberculosis* from the complete genome sequence. Nature 393:537–544. https://doi.org/10.1038/31159.
26. Gupta K, Kumar P, Chatterji D. 2010. Identification, activity and disulfide connectivity of C-di-GMP regulating proteins in *Mycobacterium tuberculosis*. PLoS One 5:e15072. https://doi.org/10.1371/journal.pone.0015072.
27. Botelho A, Canto A, Leao C, Cunha MV. 2015. Clustered regularly interspaced short palindromic repeats (CRISPRs) analysis of members of the *Mycobacterium tuberculosis* complex. Methods Mol Biol 1247:373–389. https://doi.org/10.1007/978-1-4939-2004-4_27.
28. Srivastav R, Kumar D, Grover A, Singh A, Manjasetty BA, Sharma R, Taneja B. 2014. Unique subunit packing in mycobacterial nanoRNase leads to alternate substrate recognitions in DHH phosphodiesterases. Nucleic Acids Res 42:7894–7910. https://doi.org/10.1093/nar/gku425.
29. Patterson AG, Yevstigneyeva MS, Fineran PC. 2017. Regulation of CRISPR-Cas adaptive immune systems. Curr Opin Microbiol 37:1–7. https://doi.org/10.1016/j.mib.2017.02.004.
30. Kahramanoglou C, Cortes T, Matange N, Hunt DM, Visweswariah SS, Young DB, Buxton RS. 2014. Genomic mapping of cAMP receptor protein (CRPMt) in *Mycobacterium tuberculosis*: relation to transcriptional start sites and the role of CRPMt as a transcription factor. Nucleic Acids Res 42:8320–8329. https://doi.org/10.1093/nar/gku548.
31. Knapp GS, Lyubetskaya A, Peterson MW, Gomes AL, Ma Z, Galagan JE, McDonough KA. 2015. Role of intragenic binding of cAMP responsive protein (CRP) in regulation of the succinate dehydrogenase genes Rv0249c-Rv0247c in TB complex mycobacteria. Nucleic Acids Res 43:5377–5393. https://doi.org/10.1093/nar/gkv420.
32. Rickman L, Saldanha JW, Hunt DM, Hoar DN, Colston MJ, Millar JB, Buxton RS. 2004. A two-component signal transduction system with a PAS domain-containing sensor is required for virulence of *Mycobacterium tuberculosis* in mice. Biochem Biophys Res Commun 314:259–267. https://doi.org/10.1016/j.bbrc.2003.12.082.
33. Dey A, Shree S, Pandey SK, Tripathi RP, Ramachandran R. 2016. Crystal structure of *Mycobacterium tuberculosis* H37Rv AldR (Rv2779c), a regulator of the ald gene: DNA binding and identification of small molecule inhibitors. J Biol Chem 291:11967–11980. https://doi.org/10.1074/jbc.M115.700484.
34. Parti RP, Shrivastava R, Srivastava S, Subramanian AR, Roy R, Srivastava BS, Srivastava R. 2008. A transposon insertion mutant of *Mycobacterium fortuitum* attenuated in virulence and persistence in a murine infection model that is complemented by Rv3291c of *Mycobacterium tuberculosis*. Microb Pathog 45:370–376. https://doi.org/10.1016/j.micpath.2008.08.008.
35. Shrivastava T, Dey A, Ramachandran R. 2009. Ligand-induced structural transitions, mutational analysis, and 'open' quaternary structure of the *M. tuberculosis* feast/famine regulatory protein (Rv3291c). J Mol Biol 392:1007–1019. https://doi.org/10.1016/j.jmb.2009.07.084.
36. Song N, Cui Y, Li Z, Chen L, Liu S. 2016. New targets and cofactors for the transcription factor LrpA from *Mycobacterium tuberculosis*. DNA Cell Biol 35:167–176. https://doi.org/10.1089/dna.2015.3040.
37. Gordon BR, Imperial R, Wang L, Navarre WW, Liu J. 2008. Lsr2 of Mycobacterium represents a novel class of H-NS-like proteins. J Bacteriol 190:7052–7059. https://doi.org/10.1128/JB.00733-08.
38. Gordon BR, Li Y, Wang L, Sintsova A, van Bakel H, Tian S, Navarre WW, Xia B, Liu J. 2010. Lsr2 is a nucleoid-associated protein that targets AT-rich sequences and virulence genes in *Mycobacterium tuberculosis*. Proc Natl Acad Sci U S A 107:5154–5159. https://doi.org/10.1073/pnas.0913551107.
39. Qu Y, Lim CJ, Whang YR, Liu J, Yan J. 2013. Mechanism of DNA organization by *Mycobacterium tuberculosis* protein Lsr2. Nucleic Acids Res 41:5263–5272. https://doi.org/10.1093/nar/gkt249.
40. Sharadamma N, Harshavardhana Y, Singh P, Muniyappa K. 2010. *Mycobacterium tuberculosis* nucleoid-associated DNA-binding protein H-NS binds with high-affinity to the Holliday junction and inhibits strand exchange promoted by RecA protein. Nucleic Acids Res 38:3555–3569. https://doi.org/10.1093/nar/gkq064.
41. Fang M, Zeisberg WM, Condon C, Ogryzko V, Danchin A, Mechold U. 2009. Degradation of nanoRNA is performed by multiple redundant RNases in *Bacillus subtilis*. Nucleic Acids Res 37:5114–5125. https://doi.org/10.1093/nar/gkp527.
42. Goldman SR, Sharp JS, Vvedenskaya IO, Livny J, Dove SL, Nickels BE. 2011. NanoRNAs prime transcription initiation *in vivo*. Mol Cell 42:817–825. https://doi.org/10.1016/j.molcel.2011.06.005.
43. Elmore JR, Sheppard NF, Ramia N, Deighan T, Li H, Terns RM, Terns MP. 2016. Bipartite recognition of target RNAs activates DNA cleavage by the type III-B CRISPR-Cas system. Genes Dev 30:447–459. https://doi.org/10.1101/gad.272153.115.
44. Estrella MA, Kuo FT, Bailey S. 2016. RNA-activated DNA cleavage by the type III-B CRISPR-Cas effector complex. Genes Dev 30:460–470. https://doi.org/10.1101/gad.273722.115.
45. Kazlauskiene M, Tamulaitis G, Kostiuk G, Venclovas C, Siksnys V. 2016. Spatiotemporal control of type III-A CRISPR-Cas immunity: coupling DNA degradation with the target RNA recognition. Mol Cell 62:295–306. https://doi.org/10.1016/j.molcel.2016.03.024.
46. Bai G, Schaak DD, McDonough KA. 2009. cAMP levels within *Mycobacterium tuberculosis* and *Mycobacterium bovis* BCG increase upon infection of macrophages. FEMS Immunol Med Microbiol 55:68–73. https://doi.org/10.1111/j.1574-695X.2008.00500.x.
47. Grundner C, Cox JS, Alber T. 2008. Protein tyrosine phosphatase PtpA is not required for *Mycobacterium tuberculosis* growth in mice. FEMS Microbiol Lett 287:181–184. https://doi.org/10.1111/j.1574-6968.2008.01309.x.
48. Bardarov S, Bardarov S, Jr, Pavelka MS, Jr, Sambandamurthy V, Larsen M, Tufariello J, Chan J, Hatfull G, Jacobs WR, Jr. 2002. Specialized transduction: an efficient method for generating marked and unmarked targeted gene disruptions in *Mycobacterium tuberculosis*, *M. bovis* BCG and *M. smegmatis*. Microbiology 148:3007–3017. https://doi.org/10.1099/00221287-148-10-3007.
49. Tufariello JM, Jacobs WR, Jr, Chan J. 2004. Individual *Mycobacterium tuberculosis* resuscitation-promoting factor homologues are dispensable for growth in vitro and in vivo. Infect Immun 72:515–526. https://doi.org/10.1128/IAI.72.1.515-526.2004.
50. Mangan JA, Sole KM, Mitchison DA, Butcher PD. 1997. An effective method of RNA extraction from bacteria refractory to disruption, including mycobacteria. Nucleic Acids Res 25:675–676. https://doi.org/10.1093/nar/25.3.675.
51. McClure R, Balasubramanian D, Sun Y, Bobrovskyy M, Sumby P, Genco CA, Vanderpool CK, Tjaden B. 2013. Computational analysis of bacterial RNA-Seq data. Nucleic Acids Res 41:e140. https://doi.org/10.1093/nar/gkt444.
52. Tjaden B. 2015. De novo assembly of bacterial transcriptomes from RNA-seq data. Genome Biol 16:1. https://doi.org/10.1186/s13059-014-0572-2.
53. Gazdik MA, McDonough KA. 2005. Identification of cyclic AMP-regulated genes in *Mycobacterium tuberculosis* complex bacteria under low-oxygen conditions. J Bacteriol 187:2681–2692. https://doi.org/10.1128/JB.187.8.2681-2692.2005.
54. Alland D, Kramnik I, Weisbrod TR, Otsubo L, Cerny R, Miller LP, Jacobs WR, Jr, Bloom BR. 1998. Identification of differentially expressed mRNA in prokaryotic organisms by customized amplification libraries (DECAL): the effect of isoniazid on gene expression in *Mycobacterium tuberculosis*. Proc Natl Acad Sci U S A 95:13227–13232. https://doi.org/10.1073/pnas.95.22.13227.
55. Manganelli R, Dubnau E, Tyagi S, Kramer FR, Smith I. 1999. Differential expression of 10 sigma factor genes in *Mycobacterium tuberculosis*. Mol Microbiol 31:715–724. https://doi.org/10.1046/j.1365-2958.1999.01212.x.
56. Purkayastha A, McCue LA, McDonough KA. 2002. Identification of a *Mycobacterium tuberculosis* putative classical nitroreductase gene whose expression is coregulated with that of the *acr* gene within macrophages, in standing versus shaking cultures, and under low oxygen conditions. Infect Immun 70:1518–1529. https://doi.org/10.1128/IAI.70.3.1518-1529.2002.
57. McDonough KA, Florczyk MA, Kress Y. 2000. Intracellular passage within

macrophages affects the trafficking of virulent tubercle bacilli upon reinfection of other macrophages in a serum-dependent manner. Tuber Lung Dis 80:259–271. https://doi.org/10.1054/tuld.2000.0268.
58. Vasudeva-Rao HM, McDonough KA. 2008. Expression of the *Mycobacterium tuberculosis acr*-coregulated genes from the DevR (DosR) regulon is controlled by multiple levels of regulation. Infect Immun 76:2478–2489. https://doi.org/10.1128/IAI.01443-07.
59. El Qaidi S, Yang J, Zhang JR, Metzger DW, Bai G. 2013. The vitamin B6 biosynthesis pathway in *Streptococcus pneumoniae* is controlled by pyridoxal 5′-phosphate and the transcription factor PdxR and has an impact on ear infection. J Bacteriol 195:2187–2196. https://doi.org/10.1128/JB.00041-13.
60. Ryjenkov DA, Tarutina M, Moskvin OV, Gomelsky M. 2005. Cyclic diguanylate is a ubiquitous signaling molecule in bacteria: insights into biochemistry of the GGDEF protein domain. J Bacteriol 187:1792–1798. https://doi.org/10.1128/JB.187.5.1792-1798.2005.
61. Bai Y, Yang J, Eisele LE, Underwood AJ, Koestler BJ, Waters CM, Metzger DW, Bai G. 2013. Two DHH subfamily 1 proteins in *Streptococcus pneumoniae* possess cyclic di-AMP phosphodiesterase activity and affect bacterial growth and virulence. J Bacteriol 195:5123–5132. https://doi.org/10.1128/JB.00769-13.
62. Bai Y, Yang J, Zarrella TM, Zhang Y, Metzger DW, Bai G. 2014. Cyclic di-AMP impairs potassium uptake mediated by a cyclic di-AMP binding protein in *Streptococcus pneumoniae*. J Bacteriol 196:614–623. https://doi.org/10.1128/JB.01041-13.
63. Underwood AJ, Zhang Y, Metzger DW, Bai G. 2014. Detection of cyclic di-AMP using a competitive ELISA with a unique pneumococcal cyclic di-AMP binding protein. J Microbiol Methods 107:58–62. https://doi.org/10.1016/j.mimet.2014.08.026.
64. Miller E. 2016. Rapid amplification of cDNA ends for RNA transcript sequencing in *Staphylococcus*. Methods Mol Biol 1373:169–183. https://doi.org/10.1007/7651_2015_282.
65. DiChiara JM, Contreras-Martinez LM, Livny J, Smith D, McDonough KA, Belfort M. 2010. Multiple small RNAs identified in *Mycobacterium bovis* BCG are also expressed in *Mycobacterium tuberculosis* and *Mycobacterium smegmatis*. Nucleic Acids Res 38:4067–4078. https://doi.org/10.1093/nar/gkq101.